

REPORT



Monoclonal antibody 2C5 specifically targets neutrophil extracellular traps

Livia P. Mendes^a, Kobra Rostamizadeh^b, Kandace Gollomp^c, Jacob W. Myerson^d, Oscar A. Marcos-Contreras^d, Marco Zamora^d, Ed Luther^e, Jacob S. Brenner^{d,f}, Nina Filipczak^a, Xiang Li^{a,g}, and Vladimir P. Torchilin^{a,h}

^aCenter for Pharmaceutical Biotechnology and Nanomedicine, Northeastern University, Boston, MA, USA; ^bZanjan Pharmaceutical Nanotechnology Research Center, School of Pharmacy, Pharmaceutical Biomaterials Department, Zanjan University of Medical Sciences, Zanjan, Iran; ^cDivision of Hematology, Children's Hospital of Philadelphia, Philadelphia, PA, USA; ^dDepartment of Systems Pharmacology and Translational Therapeutics, University of Philadelphia, Philadelphia, PA, USA; ^eDepartment of Pharmaceutical Sciences, Northeastern University, Boston, MA, USA; ^fPulmonary, Allergy, & Critical Care Division, University of Philadelphia, PA, USA; ^gState Key Laboratory of Innovative Drug and Efficient Energy-Saving Pharmaceutical Equipment, Jiangxi University of Traditional Chinese Medicine, Nanchang, China; ^hDepartment of Oncology, Radiotherapy and Plastic Surgery, I.M. Sechenov First Moscow State Medical University (Sechenov University), Moscow, Russia

ABSTRACT

Neutrophils can release DNA and granular cytoplasmic proteins that form smooth filaments of stacked nucleosomes (NS). These structures, called neutrophil extracellular traps (NETs), are involved in multiple pathological processes, and NET formation and removal are clinically significant. The monoclonal antibody 2C5 has strong specificity toward intact NS but not to individual NS components, indicating that 2C5 could potentially target NS in NETs. In this study, NETs were generated *in vitro* using neutrophils and HL-60 cells differentiated into granulocyte-like cells. The specificity of 2C5 toward NETs was evaluated by ELISA, which showed that it binds to NETs with the specificity similar to that for purified nucleohistone substrate. Immunofluorescence showed that 2C5 stains NETs in both static and perfused microfluidic cell cultures, even after NET compaction. Modification of liposomes with 2C5 dramatically enhanced liposome association with NETs. Our results suggest that 2C5 could be used to identify and visualize NETs and serve as a ligand for NET-targeted diagnostics and therapies.

ARTICLE HISTORY

Received 13 May 2020
Revised 3 November 2020
Accepted 10 November 2020

KEYWORDS

Neutrophil extracellular traps; monoclonal antibody; active targeting; 2C5

Introduction

Neutrophil extracellular traps (NETs) are composed of processed chromatin bound to granular and select cytoplasmic proteins that are released by neutrophils, in particular, to control microbial infections.^{1–3} NETs consist of a backbone of smooth filaments composed of stacked nucleosomes loaded with globular domains of granular proteins. Fully hydrated NETs have a web-like appearance and cover a space 10–15-fold larger than the volume of the cells from which they originate.⁴

The formation of NETs was initially thought to represent a novel cell death pathway, distinct from forms such as necrosis and apoptosis. More recently, at least two mechanisms of NET release have been recognized.⁵ One mechanism requires the lytic suicide of cells, while the other, vital NETosis, does not require the rupture of the cytoplasmic membrane.^{3,6} A variety of stimuli have been described as inductors of NETosis, including pathogens, activated platelets (in a toll-like receptor (TLR)-4-dependent mechanism), anti-neutrophil cytoplasmic antibodies, and artificial compounds such as phorbol myristate acetate (PMA) and bacterial lipopolysaccharides.^{7,8}

Although NETs were first described as a defense mechanism to trap and kill bacteria and other pathogens, they have also been implicated as key players in numerous disease states, including cancer and cardiovascular disease.^{9–11} Teijeira and

coworkers have recently shown that NETs released by tumor-associated neutrophils protect tumor cells from the immune cytotoxic effects of cytotoxic T lymphocytes and natural killer cells by preventing their direct contact. Furthermore, they observed that NET inhibition re-sensitizes the tumor cells to the immune cytotoxicity.¹² Metastatic cancer cells can induce neutrophils to form metastasis-supporting NETs. NET-like structures were observed around metastatic 4T1 cancer cells that had reached the lungs of mice.¹¹ Since nuclear chromatin bears various peptides and granule-derived proteins from parent neutrophils, sites of concentrated NETs are toxic to invading pathogens. NETs are, however, also responsible for collateral damage to the host in the setting of chronic NET or impaired NET removal.⁹ For instance, NETs are involved in acute thrombotic complications in cardiovascular and autoimmune disease,^{13–16} abnormal response to infection in systemic lupus erythematosus,¹⁷ and tumor metastasis.^{7,18–21} Moreover, excess NET formation generally jeopardizes normal endothelial function. Recent autopsy results and literature are available supporting the hypothesis that a powerful function of neutrophils – the ability to form NETs – may contribute to organ damage and mortality in COVID-19. Lung infiltration of neutrophils was shown in an autopsy specimen from a patient who succumbed to COVID-19. Targeted destruction of NETs may reduce the clinical severity of COVID-19.²²

CONTACT Vladimir P. Torchilin,  v.torchilin@northeastern.edu  Center for Pharmaceutical Biotechnology and Nanomedicine, Northeastern University, Boston, MA, USA.

 Supplemental data for this article can be accessed on the [publisher's website](#).

© 2020 The Author(s). Published with license by Taylor & Francis Group, LLC.

This is an Open Access article distributed under the terms of the Creative Commons Attribution-NonCommercial License (<http://creativecommons.org/licenses/by-nc/4.0/>), which permits unrestricted non-commercial use, distribution, and reproduction in any medium, provided the original work is properly cited.

Given the importance of NETs in a wide range of pathologies, active targeting of disease-associated NETs could be important as a diagnostic and therapeutic tool. The use of antibodies as highly specific targeting molecules can improve therapeutic outcomes relative to non-targeted drugs.^{23–25} A panel of monoclonal antibodies (mAbs) with specificity to intact nucleosomes (NS), the main component of NETs, was described and evaluated in previous studies.^{26,27} Some of these antibodies with NS-restricted specificity, such as mAb 2C5 and 1G3, were successfully used to recognize NS on the surface of NS-bearing cancer cells. These antibodies precisely targeted various drug-loaded pharmaceutical nanocarriers, including liposomes and polymeric micelles, to various tumors, confirming their excellent ability to recognize chromatin fragments.^{28–30} These studies provide a foundation to evaluate the use of these antibodies as a tool in NET-related pathologies.

The problem of NETs removal under conditions when their pathological role becomes dominant is clearly of utmost importance. The main goal of this research was to develop methods to visualize NETs, and to specifically target areas of NET accumulation using 2C5 antibody and nanocarriers functionalized with 2C5 antibody. Our NET-targeting antibody may provide substantial benefits in identifying NET-affected areas.

Results

HL-60 differentiation and characterization

To facilitate the studies of NETs and their properties, NETs or NET-like structures were generated *in vitro* by exposing the human promyelocytic leukemia cell line to dimethyl sulfoxide (DMSO) and all-trans retinoic acid (ATRA), resulting in the differentiation of these cells into granulocyte-like cells (Figure S1A, Supplementary Information).

Results from the nitro blue tetrazolium (NBT) reduction assay (Figure S1A) show that after exposure to both ATRA and DMSO for as little as 3 days, dHL-60 cells were able to reduce NBT into formazan crystals in the presence of PMA, a common characteristic of granulocytes. The extent of crystal formation was similar for both groups, which produced approximately 4-fold more formazan crystals than control HL-60 cells after 3 days of differentiation.

Differences in the morphology of HL-60 cells exposed to DMSO or ATRA after 3 days were observed (Figure S1B), although they were more pronounced in DMSO-differentiated cells. The volume of the cells decreased when incubated in the presence of both compounds. Additionally, DMSO-differentiated cells (DMSO-dHL-60) shifted to a more angular shape. The morphology changes can be followed in the time-lapse videos obtained with phase holographic imaging (See Supplementary Materials videos 1, 2, and 3 of HL-60 control, DMSO-dHL-60 and ATRA-dHL-60, respectively).

NET stimulation, visualization and quantification

Neutrophils can generate NETs *in vitro* upon stimulation with certain compounds.⁸ The web-like structures of chromatin-encompassing proteins expressed in granulocytes, such as

myeloperoxidase (MPO) and neutrophil elastase, can be visualized with fluorescent microscopy after staining the DNA and granular proteins.^{4,8,31} Differentiated HL-60 also extrude decondensed genomic DNAs into the extracellular space that are morphologically similar to NETs from neutrophils stimulated with lipopolysaccharide (LPS) or interleukin (IL)-8. Generation of NETs from both differentiated HL-60 cells and neutrophils, visualized by staining MPO, can be seen in Figure S2 (Supplementary Information). We noticed that DMSO-dHL-60 could generate more visible NETs when incubated with the calcium ionophore (CI) A18723 rather than with PMA or ATRA-dHL-60 exposed to CI or PMA (data not shown). For this reason, all subsequent assays were done using DMSO-dHL60 differentiated cells.

Quantification of NETs by fluorometric analysis was achieved by measuring the fluorescent signal of cells stimulated with CI and stained with SYTOX green, a DNA dye impermeable to live cells (Figure S3, Supplementary Information). The fluorescence observed thus represents DNA released from the cells or that of membrane-compromised cells. Figure 3(a,c) shows the kinetic pattern of the increase in green fluorescence from the groups stimulated with CI, IL-8, and LPS over 3 h. The fluorescence from the stimulated cells was clearly higher than that of non-stimulated cells, although there is some difference in the kinetic pattern for neutrophils and differentiated HL-60 cells. The use of a higher concentration of CI did not promote more DNA release. Imaging techniques were compared to the NET quantification to confirm the fluorescence signal is from generated NETs. As can be seen in Figure 3(b), following CI-stimulation of dHL-60 cells, NETs are formed (see detail in the augmented insert), but fluorescence originates from both extruded NETs and from DNA content still within the boundaries of the cell membrane. Figure 3(d) illustrates NETs formation in neutrophils following LPS stimulation. Although cells and stimulants are different, the response of the cells resulting in NETs formation seems to be very similar.

Specific activity of mAb 2C5

The enzyme-linked immunosorbent assay (ELISA) is widely used to assess the binding of antibodies to antigens immobilized on a solid surface. To verify the immunoreactivity of the 2C5 mAb against NETs in a pattern similar to nucleosomes, a NET-enriched supernatant isolated from stimulated dHL-60 was used as a substrate to coat an ELISA plate using the same procedure used for nucleohistone coating.^{32–34} Figure 1 shows that mAb 2C5 bound effectively to the NET monolayer to a degree similar to that of nucleohistones, suggesting that 2C5 presents specific activity against NETs.

2C5 binds to NETs in different *in vitro* models

Given that mAb 2C5 showed specific activity to NETs, its capacity to stain these structures for microscopy purposes was assessed. Neutrophils isolated from whole blood were activated by incubation with CI and PMA to generate NETs. As shown in Figure 2, activated neutrophils released filaments and diffuse, cloudy structures (Figure 2, arrows) that readily stained with the Hoechst DNA dye. This finding was most

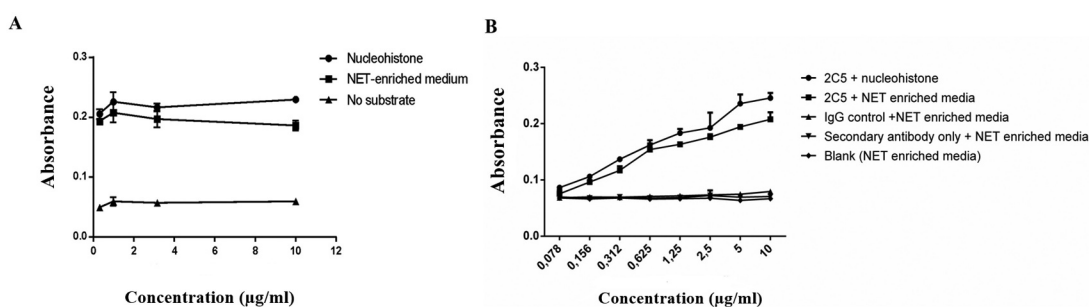


Figure 1. Immunoreactivity of mAb 2C5. Indirect ELISA was used to evaluate the binding of 2C5 antibody to a monolayer of different antigens: (a) HL-60 produced NETs and nucleohistones, (b) neutrophils produced NETs and nucleohistones. The affinity for both substrates is similar, indicating 2C5 has specific activity against NETs, as well as for nucleosomes. Detection was done using a horseradish peroxidase (HRP)-conjugated secondary antibody. Data represents the mean \pm SD, $n = 3$.

prominent in the PMA-stimulated group, although also noteworthy in CI-stimulated neutrophils. When 2C5 was added, it successfully stained NETs, showing a co-localization of 2C5 and DNA staining in the overlap images. The colocalization was assessed visually and by obtaining the Pearson's correlation coefficient (PCC) and indicates there is good correlation of pixel intensity distribution between red and blue channels in PMA – and CI-treated groups. The considerable PCC values in these groups indicate that 2C5 co-localizes with DNA in the NET structures formed upon neutrophil stimulation.

A microfluidic cell culture system was also used to evaluate 2C5 binding to NETs. Fibronectin-coated microfluidic channels were infused with neutrophils activated with tumor necrosis factor. Following channel wall adhesion, the cells were stimulated with PMA to generate NETs. NETs were stained with SYTOX orange to identify the extracellular DNA, and the channels were infused with either Alexa 488-labeled 2C5 and or isotype IgG to evaluate the antibody specificity under conditions of flow. Figure 3(a) and Video 4 (Supplementary material) show that 2C5 antibody readily binds and stains NETs, while its isotype counterpart does not bind to the extracellular chromatin. The same pattern was observed for liposomes modified with 2C5 (Figure 3(b) and Supplementary video 5), with an apparently even higher interaction than with antibody alone. The web-like structure of NETs could allow for the nonspecific capture of these macromolecules, but the specificity of 2C5 binding is clearly shown by its stronger staining signal.

To further assess if 2C5 can bind NETs under variable conditions, platelet factor 4 (PF4) was perfused in the microfluidic channels. PF4 is released by activated platelets in high concentrations at sites of thrombosis and in heparin-induced thrombocytopenia (HIT). Due to its positive charge, it binds to the extracellular DNA released by NETs, forming compact PF4-NET complexes (Figure 4). Despite these morphological changes, 2C5 binding was still achieved for both the antibody alone and the decorated liposomes, indicating that the conformational epitope required for 2C5 binding is preserved and remains available.

Discussion

Cell differentiation was assessed by distinct methods, including microscopy to observe cell morphology, a fluorescent plate assay to confirm the release of NETs, and the functional NBT

reduction assay. The latter is based on the conversion of oxygen into superoxide anion by nicotinamide adenine dinucleotide phosphate oxidase, which can then reduce NBT, leading to the formation of blue crystals.^{35,36} Other studies have similarly shown changes in the respiratory burst of differentiated cells. In these studies, however, ATRA-dHL-60 reduced NBT more efficiently than DMSO and other compounds.^{37,38} Longer incubation times did not significantly increase the generation of the crystals, indicating that 3 days are sufficient to obtain cells with neutrophil-like characteristics. After differentiation, the cells were stimulated to check their capacity to generate NETs, followed by staining for visualization. It is known, however, that only about 10% of dHL-60 can release NET-like structures after stimulation with a variety of compounds. In addition, the released structures are shorter and more discreet than the long and diffuse NETs released by neutrophils,^{39,40} a characteristic also observed in this study (Figure S2). Manda-Handzlik and coworkers showed that different agents differentiate HL-60 by distinct mechanisms, affecting their ability to generate NETs in response to various stimuli. They also found that DMSO-dHL-60 released NET-like structures only after stimulation with CI, but not with PMA.³⁸ In addition, NETs generation from neutrophils can also be induced by a variety of stimuli. Bacterial or endogenous stimuli, such as immune complexes, are known to act as triggers for NETosis. As an experimental counterpart for calcium ionophore, LPS from *E. coli* and IL-8 were used to demonstrate different pathway of NETosis.⁹

NETs were quantified by the fluorescence analysis. While this method provides insight into DNA release, it is not NET-specific,⁴¹ as CI can increase dHL-60 membrane permeability,⁴² facilitating intracellular DNA staining with SYTOX. Hence, imaging techniques were used as a confirmatory technique, showing that, although SYTOX also stained intracellular DNA in CI-stimulated cells, the formation of NET-like structures was clear (Figure S3B). Lelliott et al. recently developed an imaging flow cytometry automated analysis method to characterize and quantify NETs *in vitro* based on DNA staining.⁴³ In their study, they characterized different cell types and NET structures after exposure to NET stimulants. Besides the extracellular DNA (exDNA) and DNA fragments characteristic of NETs, they noticed the presence of SYTOX-stained cells with decondensed DNA and an absence of exDNA. They hypothesized that these cells represent another type of cell death rather than NETosis.

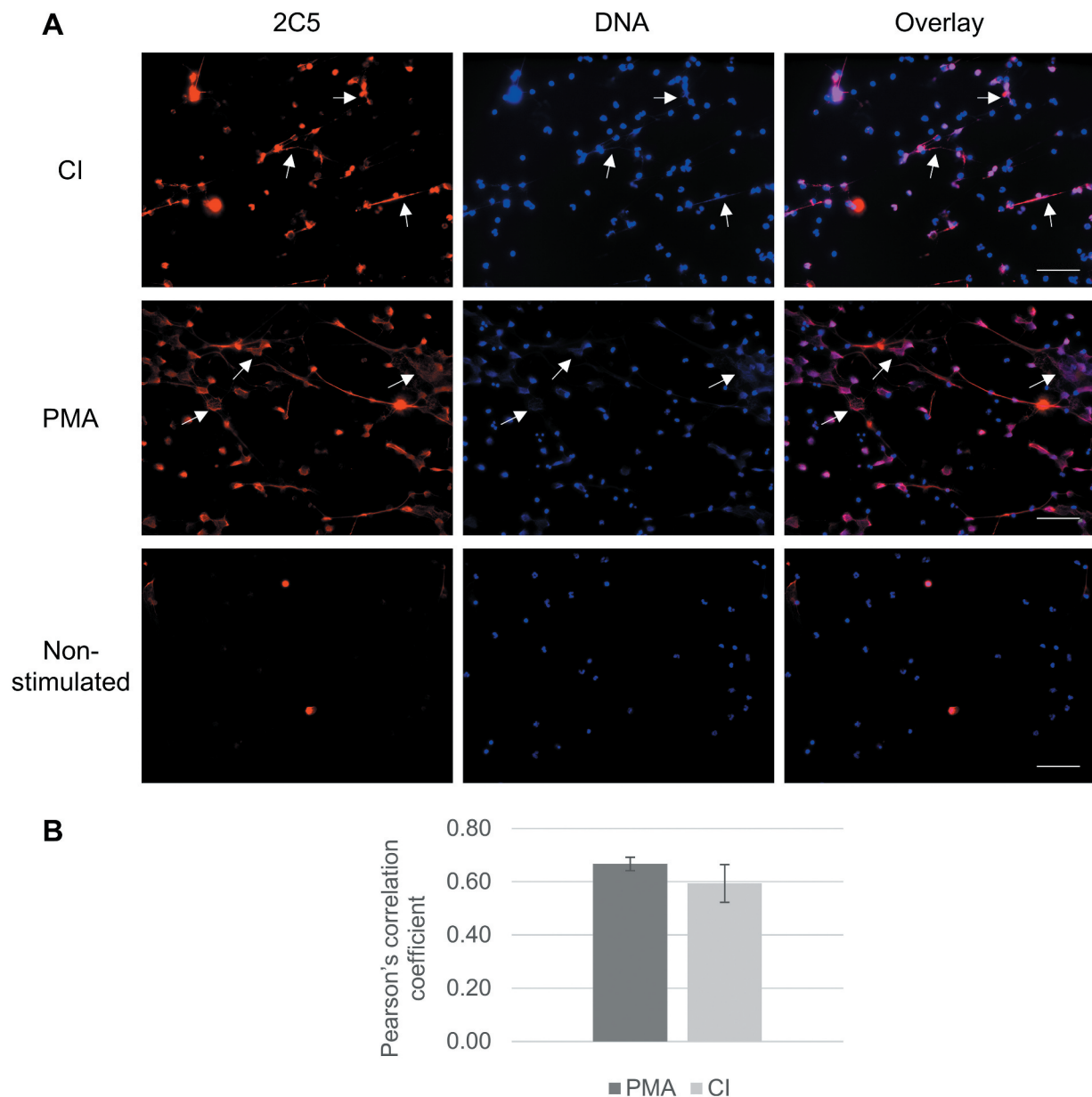


Figure 2. mAb 2C5 binding to NETs *in vitro*. (a) Neutrophils were isolated from whole blood and stimulated with either PMA or CI, followed by staining with 2C5 antibodies (red) and counterstaining using Hoechst (blue). Activated neutrophils produced NETs, confirmed by the presence of web-like structures and filamentous structures comprised of decondensed DNA (arrows). These structures were also labeled with 2C5, to show the specificity of this antibody against NETs, presenting an overlap with the DNA staining (magenta). (b) Pearson's correlation coefficient was analyzed using Image-J and indicates good correlation of pixel intensity distribution between red and blue channels in PMA and CI treated groups. The image brightness and contrast of the 2C5 channel were adjusted using the B&C tool of Image-J Software to improve visualization, especially in the overlay images. Equal adjustments were applied to images that were obtained at the same day and using the same microscope parameters. Scale bar = 50 μ m.

The specific activity of 2C5 toward NETs was evaluated in this work using ELISA, which showed that the antibody binds to NET-enriched substrate obtained from IL-8 stimulated neutrophils or CI-stimulated dHL-60 cells. mAb 2C5, which is nucleosome-specific, was previously shown to recognize only intact NS among many nuclear and other antigens, and it possessed NS-restricted specificity in ELISA when tested against artificially reconstituted NSs.^{26–28} MAbs with selective specificity for NS, i.e., to chromatin, the main component of NETs, have been described previously by Yager et al.⁴⁴ Their specificity toward NSs was clearly demonstrated in ELISAs used to test a panel of different nuclear antigens.

Additionally, in ELISA and Western blot assays with the isotype-matched UPC 10 antibody as a negative control, they did not react with such nuclear antigens as ssDNA, dsDNA, histones (individual and mixtures), H1 peptide 144–159, H1 peptide 204–218, ribonucleoprotein, La/SS-B, Ro/SS-A, Sm, Jo-1, and scl-70. The mAbs also did not react with other tested antigens, including myosin, b-galactosidase, phosphorylase b, glutamic dehydrogenase, lactate dehydrogenase, carbonic anhydrase, trypsin inhibitor, lysozyme, aprotinin, insulin, heparin, heparin sulfate, and dextran sulfate. These mAbs were shown to possess intact NS-restricted specificity in ELISA when tested against artificially reconstituted NSs,^{45,46}

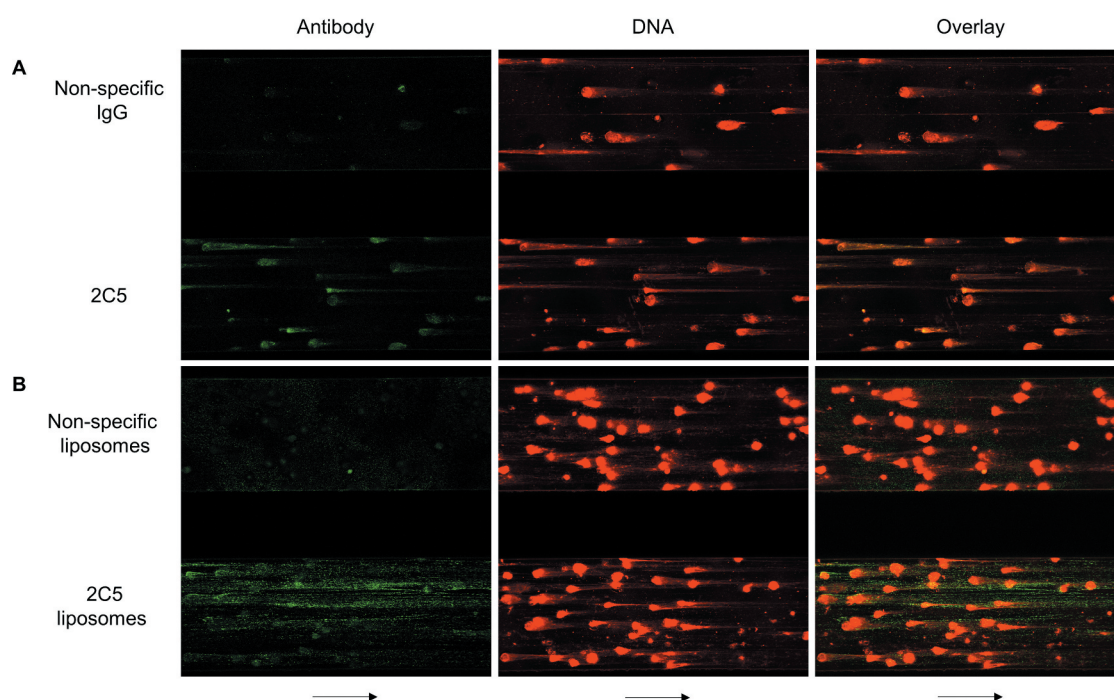


Figure 3. Microfluidic studies illustrating 2C5-NET interactions. Representative wide-field images of NETs formed in microfluidic channels, stained with SYTOX Orange (red), a DNA dye impermeable to live cells. The separate channels (included in the same visual field) were simultaneously infused at 2 dynes/cm² with Alexa 488-labeled 2C5 and non-specific IgG (green) (a) or Alexa 488-labeled liposomes modified with either 2C5 or non-specific IgG on their surface (b). Arrows represent flow direction.

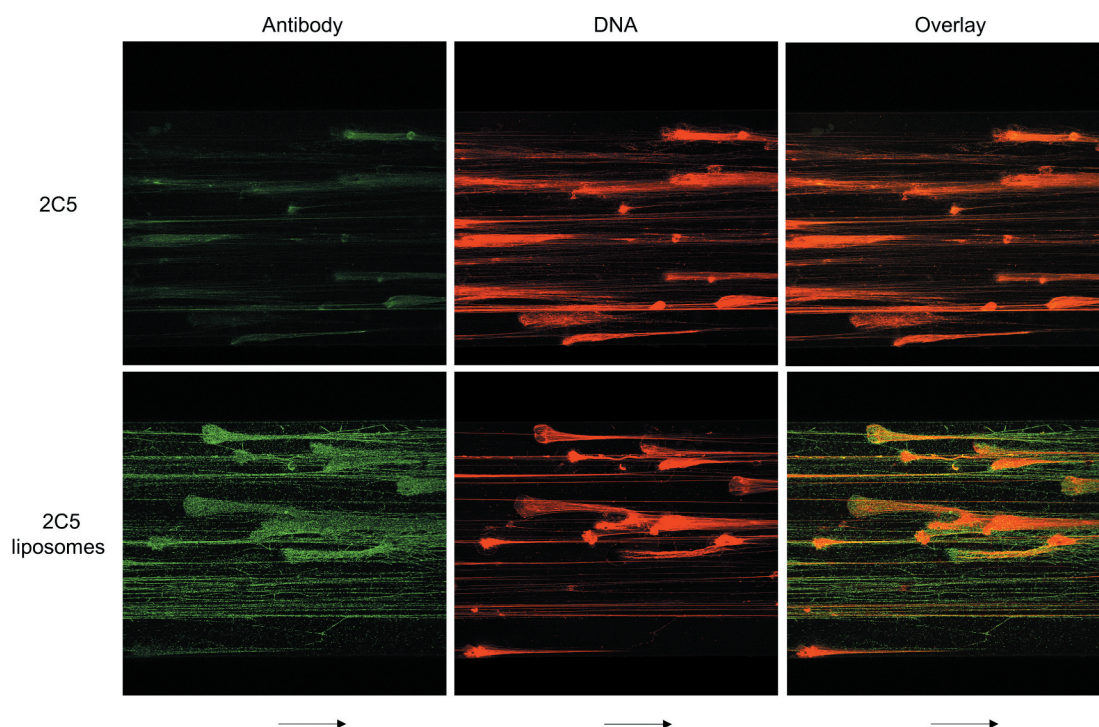


Figure 4. Morphological changes in NETs do not prevent 2C5 binding. The addition of platelet factor 4 (PF4 – a factor released by activated platelets in heparin-induced thrombocytopenia) induces chromatin compaction in NETs, as noted by reduction in NET area. PF4-NET complex formation also influences NET behavior by inducing DNase I resistance. However, 2C5 binding is not prevented, indicating that the conformational epitope required for 2C5 binding is preserved and available despite morphological changes. Arrows represent flow direction.

and did not recognize individual components of NSs, DNA and histones, or the mixture of the DNA and histones that did not contain the reconstituted NSs (a stepwise salt dialysis

procedure was not applied to DNA/histone mixture).⁴⁴ Moreover, DNase treatment eliminates mAb 2C5 binding with NS.²⁷ Control isotype-matched anti-myeloma UPC10

antibody did not react with NSs. Hence, 2C5 appears to recognize a conformational epitope of intact NS formed only by the fragments of histones 2 and 3. In ELISAs, mAb 2C5 demonstrated good binding with the mixture of histones 2 and 3 assembled on heparin (instead of DNA) (data not shown). These findings support the hypothesis that the web-like structures, composed mostly of the chromatin released from the cells, can provide the binding sites for 2C5 in NETs. Therefore, 2C5 could be used as a tool to identify and target NETs using different approaches.

The use of 2C5 as immunostaining for NETs was confirmed *in vitro* in static and perfused microfluidic cell models. NET imaging is based largely on co-staining extracellular DNA and cytoplasmic proteins bound to the chromatin, including MPO, neutrophil elastase and histone 3. Since it is known that 2C5 does not recognize individual components of NSs, including DNA and histones, its use as another staining approach to identify these structures may prove useful in other NET research fields. The microfluidic system was used in addition to the regular cell culture since the shear produced by the flow in this setup provides a different environment than that of NETs immobilized on a coverslip and can be set up to simulate flow rate as *in vivo*. In the microfluidic experiment, PF4 was added to the cells to analyze whether the formation of PF4-NET complexes, which causes NET compaction and morphological changes, impairs 2C5 binding to NETs. In addition, PF4 compaction of NETs also induces DNase I resistance,⁴⁷ which could also take advantage of the use of targeted therapy. The formation of the complexes is a finding that also occurs with multiple other cations⁴⁸ and likely influences NET behavior *in vivo*. The fact that 2C5 can still bind to NETs after these morphology changes suggests that it would be useful as a targeting moiety in drug delivery approaches for different types of NETs and for different diseases, including those associated with intense platelet activation such as HIT, disseminated intravascular coagulation, and thrombotic storm.

In conclusion, this study successfully differentiated promyelocytic leukemia cells into neutrophil-like cells, which were then used to generate NETs for *in vitro* assessment. The ability of 2C5 to bind to various NETs was confirmed by ELISA and immunostaining. Since 2C5 binds specifically to NS, its recognition of NETs is due to the presence of NS (chromatin fragments) in these structures, even after exposure to PF4, which promotes NET compaction and DNase resistance. Thus, 2C5 may potentially be used to target NETs for diagnostic purposes (visualization) when modified with appropriate labels. Furthermore, the 2C5 antibody may help control a variety of pathologies associated with NETs accumulation, such as cardiovascular, inflammatory, autoimmune, and malignant diseases, by delivering NET-targeted pharmaceutical agents, including drug-loaded nanocarriers bearing agents for NET destruction. The use of NET-targeted pharmaceutical nanocarriers could be of special importance when more than one therapeutic agent is delivered. For example, NET-driven thromboses could be treated with a combination of nucleases that cleave DNA and site-directed thrombolytic agents, optimizing thrombus digestion. The possibility of developing such systems may open new opportunities for novel approaches to the treatment of multiple pathologies.

Materials and methods

Material

Anti-MPO primary antibody (sc-51741 FITC) and a goat anti-mouse IgG-phycoerythrin-labeled secondary antibody (sc-3738) were purchased from Santa Cruz Biotechnology. Monoclonal antibody mAb 2C5 (Γ 2a; κ) was obtained by fusion of myeloma P3X63-Ag8.653 with splenocytes from two non-immunized aged mice (26 months-old BALB/c) without overt disease, produced on a commercial basis by Harlan Labs using the 2C5E3 hybridoma cell line from our lab. Horseradish peroxidase-IgG antibodies (goat anti-mouse) were purchased from Abcam (ab6789). Hoechst 33342 (H3570) was from Molecular Probes. HL-60 cells and Iscove's Modified Dulbecco's Medium (IMDM) were purchased from ATCC (ATCC[®] 30-2005[™]). Whole blood was purchased from AllCells (AllCells utilizes standardized operating procedures (SOPs) in conjunction with HIPAA compliance, state, and federal regulations. Collection protocols and donor-informed consent are subjected to the strict oversight of an Institutional Review Board (IRB). HIPAA compliance and approved protocols are followed by AllCells' collection facilities. The staff consists of highly experienced, medically licensed personnel with Medical Director oversight). Lymphocyte separation media (MT25072CI) and RPMI 1640 (MT10040CM) were acquired from Corning and red blood cell (RBC) lysis buffer 1x (00433357) was from Invitrogen. DMSO (AA439985Y) and dextran (MW 250,000 g/mol) (AAJ6020009) were from Alfa Aesar. Nitro blue tetrazolium (BP108-1) was from Fisher Scientific. Phorbol myristate acetate (NC9750026) was from LC Laboratories. All trans-retinoic acid (AC207341000) and A23187 (AC328080010) were purchased from Acros Organics. SYTOX green nucleic acid stain (S7020) was from Thermo Fisher Scientific. Recombinant human IL-8 (BD 554609) was from BD Bioscience. LPS from *E. coli* (TLRLEBLPS) was from Invivogen. Poly-L-lysine hydrobromide (MW 30,000–70,000) (P2636-25 MG) was purchased from Sigma. Calf thymus nucleohistone (LS003011) was acquired from Worthington Biochemical Corporation. 1,2-dipalmitoyl-sn-glycero-3-phosphocholine (DPPC) (850355), 1-palmitoyl-2-(dipyrrometheneboron difluoride)undecanoyl-sn-glycero-3-phosphocholine (Top fluor PC) (810281) and 1,2-distearoyl-sn-glycero-3-phosphoethanolamine-N-[azido(polyethylene glycol)-2000 (azide-terminated PEG2000-DSPE) (880228) were purchased from Avanti. All other reagents were of analytical grade.

Cell culture and differentiation

To develop an *in vitro* model of NETs, a human promyelocytic leukemia cell line, HL-60, was differentiated into neutrophil-like cells by agents, including ATRA and DMSO.³⁸ HL-60 cells were cultured using IMDM medium supplemented with 10% fetal bovine serum (FBS) and, 100 U/ml penicillin and 100 μ g/ml streptomycin were added at 37°C, 5% CO₂ and humidified air. For differentiation, these cells were exposed to ATRA and DMSO at 1 μ M and 1.25%, respectively, for 3 to 5 days. To confirm the differentiation, cells were analyzed at various time-points by the NBT reduction method,^{49,50} time-lapse phase holographic imaging⁵¹ and by brightfield microscopy (Keyence, BZ-X700, Itasca, IL, USA).

Human neutrophils were also used to produce NETs. For that, neutrophils were first isolated from whole blood⁵² using a density gradient separation technique. The use of human blood for this research was approved under institutional protocol number IBC69. Briefly, the purchased blood was collected from healthy volunteers in heparinized tubes and kept on ice until use. Blood was diluted with phosphate-buffered saline (PBS) pH 7.4 (without calcium and magnesium) and layered on top of Lymphocyte Separation Media (density 1.077 g/mL). Tubes were centrifuged at 800 x g for 30 min at 21°C. The top two layers (monocytes and lymphocytes) were removed. Dextran (MW 250,000 g/mol) was added and mixed in tubes at a final concentration of 3%. The suspension was allowed to rest for 30 min at 37°C to sediment the RBCs and the supernatant containing the granulocytes was transferred to a new tube. Tubes were centrifuged at 450 x g at 4°C for 5 minutes. The supernatant was discarded and a 1x RBC lysing solution was added to the tube to re-suspend the pellets and lyse any remaining RBCs. The tubes were kept in the dark for 10 min, centrifuged at 450 x g at 4°C for 5 min. The supernatant containing lysed RBCs was discarded. The pellet containing isolated neutrophils was washed by re-suspension in 5 mL PBS, centrifuged again, resuspended with RPMI medium supplemented with 3% FBS and used immediately.

NBT reduction assay

A quantitative NBT assay,^{35,36} with modifications, was used to determine the differentiation of HL-60 into granulocyte-like cells. Control HL-60 and cells were differentiated for different periods of time (3 to 5 days). DMSO-dHL-60 and ATRA-dHL-60 were seeded in 96-well plates (200,000 cells/well) and incubated with NBT at 1 mg/mL in the presence or absence of 10 µg/mL of PMA. After 30 min incubation, the formation of formazan crystals was observed under the microscope. The plate was centrifuged to recover the crystals, supernatant was removed, and the crystals were solubilized with DMSO. The absorbance of the solution was measured at 620 nm using a microplate reader (Synergy HT, Biotek, VT, USA) and the increase in absorbance (indicating the formation of crystals) was compared to that of control HL-60.

Phase holographic imaging

Phase holographic imaging is a laser-based methodology that captures time-lapse images of unlabeled cells and allows for observation and quantification of differences in cell morphology based on holographic reconstructions of the cells' refractive index.^{51,53} For holographic microscopy, cells were seeded on glass-bottom, 24-well plates and incubated in the presence or absence of ATRA and DMSO. The Holomonitor M4 (Phase Holographic Imaging, Lund, Sweden) was used to collect images every 10 minutes over 5 days from each well (3 regions/well) using a 20x objective lens. The data collected were analyzed using Hstudio analysis software (Phase Holographic Imaging) to characterize the morphological features of cells in the differentiation process.

NET quantification

For NET quantification, the presence of extracellular DNA was analyzed.^{4,38} Differentiated cells were seeded in 96-well plate (100,000 cells/well) and stimulated with the calcium ionophore A23187 (CI) at 4 µM and 25 µM for up to 3 hours at 37°C to induce production of NETs. The presence of extracellular DNA release was quantified by addition of 1 µM Sytox Green (DNA stain impermeant to live cells) followed by fluorometric analysis (excitation/emission: 504/523 nm) every 10 minutes. Unstimulated cells were used as controls to compare the increase in the fluorescent signal in the presence of the CI at different time points.

A similar experiment was conducted with the use of the isolated neutrophils. After seeding, neutrophils were stimulated with LPS from *E.Coli* (100 µg/ml) and IL-8 (100 ng/ml) for up to 3 hours at 37°C to induce production of NETs.

NET visualization

NETs have been described as threads of chromatin containing nuclear content and cytoplasmic proteins, including MPO and nuclease elastase.⁴ Hence, NET visualization was accomplished by immunofluorescence based on staining of the cells with antibodies against MPO and DNA. Neutrophils and HL-60 cells were seeded on glass-bottom 24-well plates and stimulated with PMA (100 nM) and CI (4 µM) for 4 hours and with LPS (100 µg/ml) and IL-8 (100 ng/ml) for 3 hours, at 37°C to induce the production of NETs. Cells were fixed with 4% paraformaldehyde, followed by blocking to prevent nonspecific binding. The plates were incubated with FITC-labeled primary anti-MPO antibody at a 1:100 dilution, washed and counterstained with Hoechst 33342 to visualize the presence of NETs released from stimulated cells. The staining patterns of PMA-, CI-, IL-8-, and LPS-stimulated cells were compared to those of unstimulated cells. In addition, live unfixed cells were labeled with Sytox Green to observe the presence of extracellular DNA release and cells with compromised cell membrane, signaled by the presence of the internalized DNA stain. The labeled plates were observed by epifluorescence microscopy (Keyence, BZ-X700). Image-J software 1.50a (NIH, Bethesda, MD) with Fiji package⁵⁴ was used to adjust the brightness and contrast of the images in the MPO channel using the B&C tool to improve visualization of the structures, especially in the overlay images. Equal adjustments were applied to images that were obtained on the same day using the same microscope parameters.

Specific activity of mAb 2C5

An ELISA was used to verify the activity of mAb 2C5 using NETs isolated from CI-stimulated HL60 cells and from IL-8 stimulated neutrophils as a substrate. For NETs isolation,^{52,55} differentiated HL60 (dHL60) in serum-free IMDM were seeded at 1.5 million cells/mL, followed by stimulation with 4 µM of CI for 4 h. Neutrophils were incubated with 100 ng/ml of IL-8 for 3 h in RPMI medium supplemented with 3% serum. The medium was gently removed, and cold PBS was added by thorough pipetting to remove any material adhered to the bottom of the flask. The suspension containing cells and

NETs was collected and centrifuged at 450 x g for 10 min at 4°C to pellet the cells. NET-enriched cell-free supernatant was collected for use as a substrate in the ELISA. For isolation of NET from stimulated neutrophils, additional centrifugation of NET-enriched cell-free supernatant was conducted as 16000 x g for 10 min at 4°C to pellet the NETs, which were used as a substrate for the ELISA. The specific activity of 2C5 has previously been verified by using nucleosomes as binding substrate.^{32–34} Briefly, an ELISA plate was first coated with poly-L-lysine (PLL). Either nucleosomes (calf thymus nucleohistone) or NET-enriched medium diluted in TBST-Casein solution were added to attach to the PLL layer and incubated for 1 h at RT. The wells were washed 3 times with TBST and a serial dilution of 2C5 was added to the wells and incubated for 1 h at RT. The samples were removed, and the wells were washed 3 times with TBST. A secondary anti-mouse horseradish peroxidase antibody was added to the plate and incubated for 2 h at RT, followed by 3-times washing of the wells. The chromogenic 3,3',5,5'-tetramethylbenzidine (TMB) substrate was added and incubated up to 15 min, followed by microplate reading at either 450 nm or 652 nm, depending on the instructions of the TMB reagent used in each assay.

Liposome preparation

Liposomes functionalized with 2C5 or isotype control IgG were prepared as previously described.⁵⁶ Lipid films were prepared by nitrogen drying and lyophilization of a mixture of chloroform solutions of DPPC:cholesterol:azide-terminated PEG₂₀₀₀-DSPE:Top Fluor PC (57.5:40:2:0.5 mol%). Dry films were hydrated with PBS and suspensions were formed via alternating bath sonication at 50°C and vortexing at room temperature. Lipid suspensions were submitted to three freeze-thaw cycles via liquid N₂ and 50°C water bath. Final suspensions were extruded through 200 nm polycarbonate filters. Liposome size and concentration following extrusion were evaluated via dynamic light scattering and NanoSight nanoparticle tracking analysis, respectively.

2C5 and isotype-matched control IgG were prepared for conjugation to azide liposomes by modification with dibenzocyclooctyne-PEG₄-n-hydroxysuccinimidyl ester (DBCO). Briefly, antibody solutions were adjusted to pH 8.3 with 1 M NaHCO₃ buffer and reacted with DBCO at a molar ratio of 1 antibody:5 DBCO for one hour at room temperature. Unreacted DBCO was removed via filtration against a 10 kDa cutoff centrifugal filter. DBCO optical absorbance (peak at 309 nm) was compared to antibody optical absorbance (shoulder at 280 nm) in order to verify DBCO conjugation to antibodies.

DBCO-modified antibodies were conjugated to azide liposomes by overnight room temperature incubation at a ratio of 200 antibody molecules per liposome. Free antibodies were separated from liposomes via size-exclusion chromatography. Liposomes were concentrated to original liposome volume with centrifugal filters and subsequently characterized with dynamic light scattering using a ZS90 Malvern Zetasizer Nano (Malvern, Westborough, MA). Liposomes had a size of 150 nm and PDI of 0.1.

2C5 staining of NETs

The ability of 2C5 to bind NETs was evaluated in two different *in vitro* models using neutrophils isolated from whole blood as described previously. In the first model, 250,000 neutrophils were seeded directly on glass coverslips (previously coated with PLL), allowed to attach for 1 h, and stimulated for 4 h with either 100 nM of PMA or 4 μM of CI in a CO₂ incubator at 37°C. Medium was removed and the cells were fixed with 4% paraformaldehyde at room temperature for 10 min, followed by permeabilization with 0.25% Triton X-100 (v/v) in PBS. After washing the cells 3 times, 5% (w/v) bovine serum albumin was added and cells were allowed to incubate overnight at 4°C. After removing the blocking solution, 2C5 primary antibody was added at 5 μg/mL and the coverslips were incubated for 1 h at room temperature. The samples were washed 3 times with PBS and a phycoerythrin-labeled goat anti-mouse antibody was added (1:200), followed by 1-hour incubation at room temperature. After washing the cells 3 times with PBS, Hoechst was added for counterstaining and the coverslips were mounted on glass slides with mounting medium. The slides were analyzed using the Keyence BZ-X700 epifluorescence microscope. Image-J with Fiji package was again used to adjust the brightness and contrast of the images in the 2C5 channel using the B&C tool to improve visualization of the structures, especially in the overlay images. Equal adjustments were applied to images that were obtained at the same day and using the same microscope parameters. In addition, the Coloc 2 plugin from Fiji was also used to analyze the images for the PCC for colocalization analysis of pixels distribution intensity between 2C5 and DNA staining.

A NET-lined microfluidic study was also performed following the procedure described previously.⁴⁷ Briefly, a BioFlux 200 Controller (Fluxion) was used and the channels were visualized with an Axio Observer Z1 inverted microscope (Zeiss) equipped with a motorized stage and an HXP-120 C metal halide illumination source. A 2 million cells/mL cell suspension was prepared using isolated neutrophils stimulated with tumor necrosis factor (Gibco, 10 ng/ml) and flowed through fibronectin-coated channels to which they adhere. The cells were incubated overnight at 37°C in the presence of 100 nM of PMA to release NETs. The channels were then flowed at 2 dynes/cm² with 1 μM of Sytox orange to stain cell-free DNA. The 2C5 antibody was conjugated to Alexa Fluor 488 using EDC-NHS synthesis. Isotype IgG was prepared in the same conditions. Samples of fluorescently labeled liposomes modified with either 2C5 or isotype IgG were used in the analysis. Both antibodies and liposomes were infused through the BioFlux channels at 2 dynes/cm² and both static images and videos were obtained. NET staining by 2C5 was analyzed using the videos in which channels with 2C5 and isotype IgG (free or conjugated to liposomes) were included in the same visual field. In addition, PF4 was infused in the channels. PF4-NET complexes show a different morphology, with compact NETs. The ability of 2C5 to bind these complexes after morphological changes was also evaluated. Images obtained as Z-stacks were processed using Image-J with Fiji package and Z-projections using maximum pixel intensity were created to better reflect the overall staining of the NETs in the plate's channels. All procedures were approved by the IRB.

Statistical analysis

Results were expressed as mean \pm standard deviation of three experiments performed independently. Analysis of variance test followed by Tukey's multiple comparisons test was used for comparison between groups unless otherwise indicated. Statistical difference was accepted when $P \leq 0.05$. Statistical analysis was done using GraphPad Prism software (version 6.01 for Windows, GraphPad Software).

Acknowledgments

We are grateful to Dr. L. Iakoubov for useful ideas.

Disclosure statement

The authors declare no conflict of interest.

Abbreviations

NET	neutrophil extracellular traps
2C5	monoclonal antibody with strong specificity towards intact nucleohistone
NBT	nitro blue tetrazolium
PMA	phorbol myristate acetate
ATRA	all-trans retinoic acid
dHL-60	HL-60 cell line differentiated into neutrophils-like cells
CI	calcium ionophore A18723
MPO	myeloperoxidase
IL-8	interleukin 8
LPS	lipopolysaccharide from <i>E. Coli</i>
mAb	monoclonal antibody

References

- Sollberger G, Tilley DO, Zychlinsky A. Neutrophil Extracellular Traps: the Biology of Chromatin Externalization. *Developmental Cell*. 2018;44:542–53. doi:10.1016/j.devcel.2018.01.019.
- Brinkmann V, Zychlinsky A. Neutrophil extracellular traps: is immunity the second function of chromatin? *The Journal of Cell Biology*. 2012;198(5):773–83. doi:10.1083/jcb.201203170.
- Nauseef WM, Kubes P. Pondering neutrophil extracellular traps with healthy skepticism. *Cellular Microbiology*. 2016;18(10):1349–57. doi:10.1111/cmi.12652.
- Brinkmann V, Reichard U, Goosmann C, Fauler B, Uhlemann Y, Weiss DS, Weinrauch Y, Zychlinsky A. Neutrophil extracellular traps kill bacteria. *Science*. 2004;303:1532. doi:10.1126/science.1092385 5663 303 1532-1535
- Douda DN, Khan MA, Grasemann H, Palaniyar N. SK3 channel and mitochondrial ROS mediate NADPH oxidase-independent NETosis induced by calcium influx. *Proc Natl Acad Sci U S A*. 2015;112:2817–22. doi:10.1073/pnas.1414055112.
- Yipp BG, Kubes P. NETosis: how vital is it? *Blood*. 2013;122(16):2784–94. doi:10.1182/blood-2013-04-457671.
- Erpenbeck L, Schon MP. Neutrophil extracellular traps: protagonists of cancer progression? *Oncogene*. 2017;36(18):2483–90. doi:10.1038/onc.2016.406.
- Hoppenbrouwers T, Autar ASA, Sultan AR, Abraham TE, van Cappellen WA, Houtsmuller AB, van Wamel WJB, van Beusekom HMM, van Neck JW, de Maat MPM. In vitro induction of NETosis: comprehensive live imaging comparison and systematic review. *PLoS One*. 2017;12:e0176472
- Papayannopoulos V. Neutrophil extracellular traps in immunity and disease. *Nature Reviews Immunology*. 2017;18:134. doi:10.1038/nri.2017.105.
- Jimenez-Alcazar M, Rangaswamy C, Panda R, Bitterling J, Simsek YJ, Long AT, Bilyy R, Krenn V, Renné C, Renné T, et al. Host DNases prevent vascular occlusion by neutrophil extracellular traps. *Science*. 2017;358:1202–06. doi:10.1126/science.aam8897.
- Park J, Wysocki RW, Amoozgar Z, Maiorino L, Fein MR, Jorns J, Schott AF, Kinugasa-Katayama Y, Lee Y, Won NH, et al. Cancer cells induce metastasis-supporting neutrophil extracellular DNA traps. *Science Translational Medicine*. 2016;8(361):361ra138. doi:10.1126/scitranslmed.aag1711.
- Teijeira Á, Garasa S, Gato M, Alfaro C, Migueliz I, Cirella A, de Andrea C, Ochoa MC, Otano I, Etxeberria I, et al. CXCR1 and CXCR2 chemokine receptor agonists produced by tumors induce neutrophil extracellular traps that interfere with immune cytotoxicity. *Immunity*. 2020;52(5):856–71.e8. doi:10.1016/j.immuni.2020.03.001.
- Franck G, Mawson TL, Folco EJ, Molinaro R, Ruvkun V, Engelbertsen D, Liu X, Tesmenitsky Y, Shvartz E, Sukhova GK, et al. Roles of PAD4 and NETosis in experimental atherosclerosis and arterial injury: implications for superficial erosion. *Circ Res*. 2018;123(1):33–42. doi:10.1161/CIRCRESAHA.117.312494.
- Qi H, Yang S, Zhang L. Neutrophil extracellular traps and endothelial dysfunction in atherosclerosis and thrombosis. *Frontiers in Immunology*. 2017;8:928. doi:10.3389/fimmu.2017.00928.
- Wang Y, Luo L, Braun OO, Westman J, Madhi R, Herwald H, Mörgelin M, Thorlacius H. Neutrophil extracellular trap-microparticle complexes enhance thrombin generation via the intrinsic pathway of coagulation in mice. *Scientific Reports*. 2018;8:4020. doi:10.1038/s41598-018-22156-5.
- Pertwi KR, van der Wal AC, Pabittei DR, Mackaaij C, van Leeuwen MB, Li X, de Boer O. Neutrophil extracellular traps participate in all different types of thrombotic and haemorrhagic complications of coronary atherosclerosis. *Thrombosis and Haemostasis*. 2018;118(6):1078–87. doi:10.1055/s-0038-1641749.
- Hakkim A, Furnrohr BG, Amann K, Laube B, Abed UA, Brinkmann V, Herrmann M, Voll RE, Zychlinsky A. Impairment of neutrophil extracellular trap degradation is associated with lupus nephritis. *Proc Natl Acad Sci U S A*. 2010;107(21):9813–18. doi:10.1073/pnas.0909927107.
- Albregues J, Shields MA, Ng D, Park CG, Ambrico A, Poindexter ME, Upadhyay P, Uyeminami DL, Pommier A, Küttner V. Neutrophil extracellular traps produced during inflammation awaken dormant cancer cells in mice. *Science*. 2018;361(6409):ea40227. doi:10.1126/science.aao4227.
- Demers M, Krause DS, Schatzberg D, Martinod K, Voorhees JR, Fuchs TA, Scadden DT, Wagner DD. Cancers predispose neutrophils to release extracellular DNA traps that contribute to cancer-associated thrombosis. *Proceedings of the National Academy of Sciences*. 2012;109(32):13076. doi:10.1073/pnas.1200419109.
- Demers M, Wong SL, Martinod K, Gallant M, Cabral JE, Wang Y, Wagner DD. Priming of neutrophils toward NETosis promotes tumor growth. *Oncoimmunology*. 2016;5(5):e1134073. doi:10.1080/2162402X.2015.1134073.
- Wen F, Shen A, Choi A, Gerner EW, Shi J. Extracellular DNA in pancreatic cancer promotes cell invasion and metastasis. *Cancer Research*. 2013;73(14):4256–66. doi:10.1158/0008-5472.CAN-12-3287.
- Barnes BJ, Adrover JM, Baxter-Stoltzfus A, Borczuk A, Cools-Lartigue J, Crawford JM, Daßler-Plenker J, Guerci P, Huynh C, Knight JS. Targeting potential drivers of COVID-19: neutrophil extracellular traps. *J Exp Med*. 2020;217(6):e20200652. doi:10.1084/jem.20200652.
- Koshkaryev A, Sawant R, Deshpande M, Torchilin V. Immunoconjugates and long circulating systems: origins, current state of the art and future directions. *Advanced Drug Delivery Reviews*. 2013;65(1):24–35. doi:10.1016/j.addr.2012.08.009.
- Gupta B, Levchenko TS, Mongayt DA, Torchilin VP. Monoclonal antibody 2C5-mediated binding of liposomes to brain tumor cells in vitro and in subcutaneous tumor model in vivo. *Journal of Drug Targeting*. 2005;13:337–43.

25. Carter T, Mulholland P, Chester K. Antibody-targeted nanoparticles for cancer treatment. *Immunotherapy*. 2016;8(8):941–58. doi:10.2217/imt.16.11.
26. Iakoubov L, Rokhlin O, Torchilin V. Anti-nuclear autoantibodies of the aged reactive against the surface of tumor but not normal cells. *Immunol Lett*. 1995;47(1–2):147–49. doi:10.1016/0165-2478(95)00066-E.
27. Iakoubov LZ, Torchilin VP. A novel class of antitumor antibodies: nucleosome-restricted antinuclear autoantibodies (ANA) from healthy aged nonautoimmune mice. *Oncology Research*. 1997;9:439–46.
28. Torchilin VP, Lukyanov AN, Gao Z, Papahadjopoulos-Sternberg B. Immunomicelles: targeted pharmaceutical carriers for poorly soluble drugs. *Proc Natl Acad Sci U S A*. 2003;100(10):6039–44. doi:10.1073/pnas.0931428100.
29. Elbayoumi TA, Torchilin VP. Tumor-specific anti-nucleosome antibody improves therapeutic efficacy of doxorubicin-loaded long-circulating liposomes against primary and metastatic tumor in mice. *Mol Pharm*. 2009;6(1):246–54. doi:10.1021/mp8001528.
30. Erdogan S, Roby A, Torchilin VP. Enhanced tumor visualization by gamma-scintigraphy with ¹¹¹In-labeled polychelating-polymer-containing immunoliposomes. *Mol Pharm*. 2006;3:525–30. doi:10.1021/mp060055t.
31. Brinkmann V, Laube B, Abu Abed U, Goosmann C, Zychlinsky A. Neutrophil extracellular traps: how to generate and visualize them. *JoVE*. 2010;36:e1724
32. Torchilin VP, Levchenko TS, Lukyanov AN, Khaw BA, Klibanov AL, Rammohan R, Samokhin GP, Whiteman KR. p-Nitrophenylcarbonyl-PEG-PE-liposomes: fast and simple attachment of specific ligands, including monoclonal antibodies, to distal ends of PEG chains via p-nitrophenylcarbonyl groups. *Biochimica Et Biophysica Acta (BBA) - Biomembranes*. 2001;1511(2):397–411. doi:10.1016/S0005-2728(01)00165-7.
33. Lukyanov AN, Elbayoumi TA, Chakilam AR, Torchilin VP. Tumor-targeted liposomes: doxorubicin-loaded long-circulating liposomes modified with anti-cancer antibody. *Journal of Controlled Release*. 2004;100(1):135–44. doi:10.1016/j.jconrel.2004.08.007.
34. Koren E, Apte A, Jani A, Torchilin VP. Multifunctional PEGylated 2C5-immunoliposomes containing pH-sensitive bonds and TAT peptide for enhanced tumor cell internalization and cytotoxicity. *J Control Release*. 2012;160(2):264–73. doi:10.1016/j.jconrel.2011.12.002.
35. Choi HS, Kim JW, Cha YN, Kim C. A quantitative nitroblue tetrazolium assay for determining intracellular superoxide anion production in phagocytic cells. *Journal of Immunoassay & Immunochemistry*. 2006;27:31–44. doi:10.1080/15321810500403722.
36. Racanicchi L, Montanucci P, Basta GP, Pensato A, Conti V, Calafiore R. Effect of all trans retinoic acid on lysosomal alpha-D-mannosidase activity in HL-60 cell: correlation with HL-60 cells differentiation. *Molecular and Cellular Biochemistry*. 2008;308:17–24. doi:10.1007/s11010-007-9606-3.
37. Sham RL, Phatak PD, Belanger KA, Packman CH. Functional properties of HL60 cells matured with all-trans-retinoic acid and DMSO: differences in response to interleukin-8 and fMLP. *Leukemia Research*. 1995;19:1–6. doi:10.1016/0145-2126(94)00063-G.
38. Manda-Handzik A, Bystrzycka W, Wachowska M, Sieczkowska S, Stelmaszczyk-Emmel A, Demkow U, Ciepiela O. The influence of agents differentiating HL-60 cells toward granulocyte-like cells on their ability to release neutrophil extracellular traps. *Immunology & Cell Biology*. 2018;96:413–25. doi:10.1111/imcb.12015.
39. Yaseen R, Blodkamp S, Lüthje P, Reuner F, Völlger L, Naim HY, von Köckritz-blickwede M. Antimicrobial activity of HL-60 cells compared to primary blood-derived neutrophils against *Staphylococcus aureus*. *J Negat Results Biomed*. 2017;16:2. doi:10.1186/s12952-017-0067-2.
40. Wang Y, Li M, Stadler S, Correll S, Li P, Wang D, Hayama R, Leonelli L, Han H, Grigoryev SA. Histone hypercitrullination mediates chromatin decondensation and neutrophil extracellular trap formation. *The Journal of Cell Biology*. 2009;184(2):205–13. doi:10.1083/jcb.200806072.
41. van der Linden M, Westerlaken GHA, van der Vlist M, van Montfrans J, Meyaard L. Differential signalling and kinetics of neutrophil extracellular trap release revealed by quantitative live imaging. *Scientific Reports*. 2017;7:6529. doi:10.1038/s41598-017-06901-w.
42. Jiang Z, Yin X, Jiang Q. Natural forms of vitamin E and 13'-carboxychromanol, a long-chain vitamin E metabolite, inhibit leukotriene generation from stimulated neutrophils by blocking calcium influx and suppressing 5-lipoxygenase activity, respectively. *Journal of Immunology*. 2011;186:1173–79. doi:10.4049/jimmunol.1002342.
43. Lelliott PM, Momota M, Lee MSJ, Kuroda E, Iijima N, Ishii KJ, Coban C. Rapid quantification of NETs in vitro and in whole blood samples by imaging flow cytometry. *Cytometry Part A*. 2019;95:565–78. doi:10.1002/cyto.a.23767
44. Yager TD, McMurray CT, Van Holde KE. Salt-induced release of DNA from nucleosome core particles. *Biochemistry*. 1989;28:2271–81. doi:10.1021/bi00431a045.
45. Peterson CL. Salt gradient dialysis reconstitution of nucleosomes. *CSH Protocols*. 2008;2008:pdb.prot5113.
46. Lee KM, Narlikar G. 2001. Assembly of nucleosomal templates by salt dialysis. *Curr Protoc Mole Biol*. 54: 21.6.1–21.6.16
47. Gollomp K, Kim M, Johnston I, Hayes V, Welsh J, Arepally GM, Kahn M, Lambert MP, Cuker A, Cines DB, et al. Neutrophil accumulation and NET release contribute to thrombosis in HIT. *JCI Insight*. 2018;3. doi:10.1172/jci.insight.99445.
48. Lande R, Botti E, Jandus C, Dojcinovic D, Fanelli G, Conrad C, Chamilos G, Feldmeyer L, Marinari B, Chonet S, et al. The antimicrobial peptide LL37 is a T-cell autoantigen in psoriasis. *Nat Commun*. 2014;5:5621. doi:10.1038/ncomms6621
49. Blair OC, Carbone R, Sartorelli AC. Differentiation of HL-60 promyelocytic leukemia cells monitored by flow cytometric measurement of nitro blue tetrazolium (NBT) reduction. *Cytometry*. 1985;6:54–61. doi:10.1002/cyto.990060110.
50. Jian P, Li ZW, Fang TY, Jian W, Zhuan Z, Mei LX, Yan WS, Jian N. Retinoic acid induces HL-60 cell differentiation via the upregulation of miR-663. *Journal of Hematology & Oncology*. 2011;4:20. doi:10.1186/1756-8722-4-20.
51. Luther E, Mendes LP, Pan J, Costa DF, Torchilin VP. Applications of label-free, quantitative phase holographic imaging cytometry to the development of multi-specific nanoscale pharmaceutical formulations. *Cytometry Part A*. 2017;91:412–23. doi:10.1002/cyto.a.23102.
52. Najmeh S, Cools-Lartigue J, Giannias B, Spicer J, Ferri LE. Simplified Human Neutrophil Extracellular Traps (NETs) isolation and handling. *Journal of Visualized Experiments*. 2015;98:52687.
53. Zhang Y, Sriraman SK, Kenny HA, Luther E, Torchilin V, Lengyel E. Reversal of chemoresistance in ovarian cancer by co-delivery of a P-Glycoprotein inhibitor and paclitaxel in a liposomal platform. *Molecular Cancer Therapeutics*. 2016;15:2282. doi:10.1158/1535-7163.MCT-15-0986.
54. Schindelin J, Arganda-Carreras I, Frise E, Kaynig V, Longair M, Pietzsch T, Preibisch S, Rueden C, Saalfeld S, Schmid B. Fiji: an open-source platform for biological-image analysis. *Nature Methods*. 2012;9(7):676–82. doi:10.1038/nmeth.2019.
55. Zou Y, Chen X, Xiao J, Bo Zhou D, Xiao LX, Li W, Xie B, Kuang X, Chen Q. Neutrophil extracellular traps promote lipopolysaccharide-induced airway inflammation and mucus hypersecretion in mice. *Oncotarget*. 2018;9(17):13276–86. doi:10.18632/oncotarget.24022.
56. Hood ED, Greineder CF, Shuvaeva T, Walsh L, Villa CH, Muzykantov VR. Vascular targeting of radiolabeled liposomes with bio-orthogonally conjugated ligands: single chain fragments provide higher specificity than antibodies. *Bioconjugate Chemistry*. 2018;29:3626–37. doi:10.1021/acs.bioconjchem.8b00564.